Development and Disintegration of Maya Political Systems in Response to Climate Change

Douglas J. Kennett *et al.*

Science **338**, 788 (2012);
DOI: 10.1126/science.1226299

Science (print ISSN 0036-8075; online ISSN 1095-9203) is published weekly, except the last week in December, by the American Association for the Advancement of Science, 1200 New York Avenue NW, Washington, DC 20005.

deposited mineral phases within fissures and cracks. The martian weathering products are the most likely source of the required LREE, incompatible, and volatile elements. Upon impact, preferential, shock-induced melting occurred in the target rock along fractures where weathering products were concentrated. This melting produced the black glass and retained in it chemical signatures characteristic of the martian surface. Shock melting also trapped a component derived from the martian atmosphere, as revealed by stepped combustion–mass spectrometry. About 0.7 My ago, the sample was ejected from Mars and eventually landed on Earth in July 2011. The martian weathering features in Tissint described here are compatible with spacecraft observations on Mars, including those made by the NASA Viking landers, MER Spirit rover, and ESA's Mars Express orbiter (*5*, *21*–*23*).

References and Notes

1. D. D. Bogard, P. Johnson, *Science* **221**, 651 (1983).
2. R. H. Becker, R. O. Pepin, *Earth Planet. Sci. Lett.* **69**, 225 (1984).
3. A. H. Treiman, J. D. Gleason, D. D. Bogard, *Planet. Space Sci.* **48**, 1213 (2000).
4. G. Crozaz, M. Wadhwa, *Geochim. Cosmochim. Acta* **65**, 971 (2001).
5. Supplementary materials are available on *Science* Online.
6. P. Rochette *et al.*, *Meteorit. Planet. Sci.* **40**, 529 (2005).
7. A. O. Nier, M. B. McElroy, *J. Geophys. Res.* **82**, 4341 (1977).
8. I. A. Franchi, I. P. Wright, A. S. Sexton, C. T. Pillinger, *Meteorit. Planet. Sci.* **34**, 657 (1999).
9. J. Blichert-Toft, J. D. Gleason, P. Télouk, F. Albarède, *Earth Planet. Sci. Lett.* **173**, 25 (1999).
10. G. Dreibus *et al.*, *Meteorit. Planet. Sci.* **35**, A49 (2000).
11. J. A. Barrat, J. Blichert-Toft, R. W. Nesbitt, F. Keller, *Meteorit. Planet. Sci.* **36**, 23 (2001).
12. C. R. Neal, L. A. Taylor, J. C. Ely, J. C. Jain, M. A. Nazarov, *Lunar Planet. Sci.* **32**, 1671 (2001).
13. B. Marty, K. Hashizume, M. Chaussidon, R. Wieler, *Space Sci. Rev.* **106**, 175 (2003).
14. T. Owen *et al.*, *J. Geophys. Res.* **82**, 4635 (1977).
15. J.-A. Barrat *et al.*, *Geochim. Cosmochim. Acta* **66**, 3505 (2002).
16. V. Sautter *et al.*, *Earth Planet. Sci. Lett.* **195**, 223 (2002).
17. P. Beck *et al.*, *Geochim. Cosmochim. Acta* **70**, 2127 (2006).
18. D. W. Mittlefehldt, M. M. Lindstrom, *Geochim. Cosmochim. Acta* **67**, 1911 (2003).
19. M. N. Rao, L. E. Borg, D. S. McKay, S. J. Wentworth, *Geophys. Res. Lett.* **26**, 3265 (1999).
20. E. L. Walton, P. J. Jugo, C. D. K. Herd, M. Wilke, *Geochim. Cosmochim. Acta* **74**, 4829 (2010).
21. R. E. Arvidson, J. L. Gooding, H. J. Moore, *Rev. Geophys.* **27**, 39 (1989).
22. L. A. Haskin *et al.*, *Nature* **436**, 66 (2005).
23. A. Gendrin *et al.*, *Science* **307**, 1587 (2005).
24. J. A. Barrat *et al.*, *Geochim. Cosmochim. Acta* **83**, 79 (2012).
25. K. Marti, J. S. Kim, A. N. Thakur, T. J. McCoy, K. Keil, *Science* **267**, 1981 (1995).

Acknowledgments: We acknowledge D. N. Menegas and family for their generous donation enabling the acquisition of Tissint (BM.2012,M1), M. Aoudjehane for fieldwork, A. Aaranson for field information, J. Gibson for assistance with oxygen isotope analysis, L. Labenne for loan of a sample, and A. Irving for 400 mg of powdered sample. This study was funded at Hassan II University Casablanca, Faculté des Sciences Ain Chock, by Centre de Recherches Scientifiques et Techniques Morocco and CNRS France (Projet International de Coopération Scientifique, Sciences de l'Univers 01/10), and by Comité Mixte Inter Universitaire Franco-Marocain Volubilis (MA/11/252); CRPG Nancy, France, by the CNES, CNRS, and European Research Council under the European Community's Seventh Framework Programme (FP7/2007-2013 no. 267255); Université de Bretagne Occidentale–Institut Universitaire Européen de la Mer, Plouzané, France, by the Programme National de Planétologie, Institut National des Sciences de l'Univers; Open University, by Science and Technology Facilities Council grant to the Planetary and Space Sciences Discipline; and University of Alberta, by the Natural Sciences and Engineering Research Council of Canada (grant 261740-03).

Supplementary Materials

www.sciencemag.org/cgi/content/full/science.1224514/DC1
Materials and Methods
Supplementary Text
Figs. S1 to S11
Tables S1 to S13
References (*26*–*35*)

9 May 2012; accepted 25 September 2012
Published online 11 October 2012;
10.1126/science.1224514

Development and Disintegration of Maya Political Systems in Response to Climate Change

Douglas J. Kennett,[1]*† Sebastian F. M. Breitenbach,[2]* Valorie V. Aquino,[3] Yemane Asmerom,[4] Jaime Awe,[5] James U.L. Baldini,[6] Patrick Bartlein,[7] Brendan J. Culleton,[1] Claire Ebert,[1] Christopher Jazwa,[1] Martha J. Macri,[8] Norbert Marwan,[9] Victor Polyak,[4] Keith M. Prufer,[3] Harriet E. Ridley,[6] Harald Sodemann,[10] Bruce Winterhalder,[11] Gerald H. Haug[2]

The role of climate change in the development and demise of Classic Maya civilization (300 to 1000 C.E.) remains controversial because of the absence of well-dated climate and archaeological sequences. We present a precisely dated subannual climate record for the past 2000 years from Yok Balum Cave, Belize. From comparison of this record with historical events compiled from well-dated stone monuments, we propose that anomalously high rainfall favored unprecedented population expansion and the proliferation of political centers between 440 and 660 C.E. This was followed by a drying trend between 660 and 1000 C.E. that triggered the balkanization of polities, increased warfare, and the asynchronous disintegration of polities, followed by population collapse in the context of an extended drought between 1020 and 1100 C.E.

The Classic Maya (300 to 1000 C.E.) left a remarkable historical record inscribed on well-dated stone monuments. Wars, marriages, and accessions of kings and queens are tied to long count calendar dates and correlate with specific days in the Christian calendar (Goodman-Thompson-Martinez correlation). The termination of this tradition between 800 and 1000 C.E. marks the widespread collapse of Classic Maya political systems. Multidecadal drought has been implicated, but remains controversial because of dating uncertainties and insufficient temporal resolution in paleoclimatic records. Lake sediments from the Yucatan Peninsula provided the first evidence of substantial drying in the Terminal Classic (*1*). However, disturbances to lake sediment sequences caused by prehistoric deforestation and agricultural expansion during the Classic Period complicate reproducing these results near the largest and most politically important Maya centers (such as Tikal and Caracol). Several studies more distant from the Maya lowlands (ML) support either relatively dry conditions or a series of droughts during the Terminal Classic (*2*–*5*), but the relevance of these records for the ML remains unclear (*6*).

Cave deposits in the ML show great promise for paleoclimatic reconstruction (*7*–*9*). The challenge lies in developing long, continuous records from rapidly growing stalagmites that can be dated precisely by using ^{234}U-^{230}Th (U-Th). Here, we present a subannually resolved rainfall record from an exceptionally well-dated stalagmite collected from Yok Balum (YB) Cave in Belize (16°12'30.780" N, 89°4'24.420" W, 366 m above sea level) (*10*). YB cave is located 1.5 km from the Classic Period Maya site of Uxbenká. Three other important Maya centers (Pusilha, Lubaantun, Nim Li Punit) are within 30 km (fig. S1); Tikal and other major Classic Period population centers (such as Caracol, Copan, and Calakmul) are

[1]Department of Anthropology, Pennsylvania State University, University Park, PA 16802, USA. [2]Department of Earth Science, Eidgenössische Technische Hochschule (ETH), CH-8092 Zürich, Switzerland. [3]Department of Anthropology, University of New Mexico, Albuquerque, NM 87131, USA. [4]Department of Earth and Planetary Sciences, University of New Mexico, Albuquerque, NM 87131, USA. [5]Institute of Archaeology, National Institute of Culture and History, Belmopan, Belize. [6]Department of Earth Sciences, University of Durham, Durham DH1 3LE, UK. [7]Department of Geography, University of Oregon, Eugene, OR 97403, USA. [8]Department of Native American Studies, University of California, Davis, Davis, CA 95616, USA. [9]Potsdam Institute for Climate Impact Research, Post Office Box 60 12 03, 14412 Potsdam, Germany. [10]Institute for Atmospheric and Climate Science, ETH, CH-8092 Zürich, Switzerland. [11]Department of Anthropology, University of California, Davis, Davis, CA 95616, USA.

*These authors contributed equally to this work.
†To whom correspondence should be addressed. E-mail: djk23@psu.edu

within 200 km and are influenced by the same climate systems (fig. S8). Age control of our climate reconstruction is comparable in precision with the historical record, providing a foundation for examining the complex nature of political dynamics in response to climate change.

In 2006, we collected a 56-cm-long stalagmite (YOK-I) from 50 m inside the western entrance of the cave (figs. S2 and S3). Forty U-Th dates indicate that the upper 415 mm of the stalagmite grew continuously between 40 B.C.E. and 2006 C.E. (table S2 and fig. S4). Analytical precision for the U-Th dates ranges from ±1 to ±17 years, and time averaging related to sample drilling is ~20 years (table S3 and fig. S5). The climate record is based on >4200 oxygen isotope ($\delta^{18}O$) measurements taken continuously in 0.1-mm increments, representing a mean temporal resolution of 0.5 years (table S4 and fig. S6). Monitoring data from YB cave combined with Hendy tests on stalagmite and glass drip plate carbonate indicate that $\delta^{18}O$ values reflect rainfall amount above the cave and that minor kinetic effects exist that increase $\delta^{18}O$ values, possibly enhancing the signal when climate conditions are dry (figs. S9 to S14). The $\delta^{18}O$ record ranges from –5.2 to –2.5 per mil (‰) and oscillates on decadal to multicentennial scales (Fig. 1). Multidecadal droughts occur between ~200 to 300, 820 to 870, 1020 to 1100, and 1530 to 1580 C.E., and the high-resolution YOK-I record permits the identification of other shorter and occasionally very severe droughts, particularly centered on AD 420, 930, and 1800. The $\delta^{18}O$ record is considered unreliable in the 20th century and not a reflection of drought conditions (fig. S7) (*10*).

We argue that climate variability was predominantly driven by Intertropical Convergence Zone (ITCZ) migration and changes in El Niño frequency, the linkage being a general perturbation of tropical climate (Walker Circulation) accompanying El Niño–Southern Oscillation (ENSO)–time scale variability. During El Niño years, the ITCZ is positioned over the eastern equatorial Pacific, and boreal summer moisture delivery to the ML decreases (*11*). Strengthened vertical wind shear linked to ITCZ position during El Niño years reduces the number of tropical depressions, storms, and hurricanes crossing the ML. Power spectral analyses of the YOK-I $\delta^{18}O$ record shows statistically significant periodicities centered on 3 to 8 years, which is consistent with a strong ENSO signal (fig. S15). Previous research used titanium concentrations in marine sediments from the Cariaco Basin to reconstruct ITCZ-related rainfall changes over the ML (*2*, *11*). We tuned the past 2000 years of the Cariaco Ti chronology within that record's errors using our high-precision U-Th chronology (Fig. 1B and fig. S16). A correlation may exist between the YOK-I $\delta^{18}O$ record and other lower-resolution records from the ML, including Lake Chichancanab sediment density record (Fig. 1C) (*12*), Lake Punta Laguna ostracod $\delta^{18}O$ record (Fig. 1D) (*13*), and the Macal Chasm speleothem luminescence record (Fig. 1E) (*8*). However, statistically significant correlations between these records are difficult to demonstrate because the chronological uncertainties of older records allow for a range of correlation coefficients. Given these uncertainties, we cannot definitively link these regional records, but visually similar trends are evident on multidecadal time scales (fig. S17).

We hypothesize that precipitation-induced changes in agricultural productivity mediated the tendency toward political integration or disintegration in the ML. Droughts recorded in the Yucatan between 1535 and 1575 C.E. (*14*) correspond to one of four multidecadal droughts evident in the YOK-I record (Fig. 2). The interval from 1535 to 1542 C.E. was particularly dry. Historical accounts link this drought to reduced agricultural productivity, famine, disease, death, and population relocation. Some estimates suggest that drought-related agricultural disaster caused nearly a million deaths in Mexico in 1535 C.E. (*15*), illustrating how meteorologically dry conditions presage agricultural drought with severe effects scaled to population density and level of agricultural intensification.

A dry period comparable with the historical drought of 1535 C.E. is evident in the YOK-I record

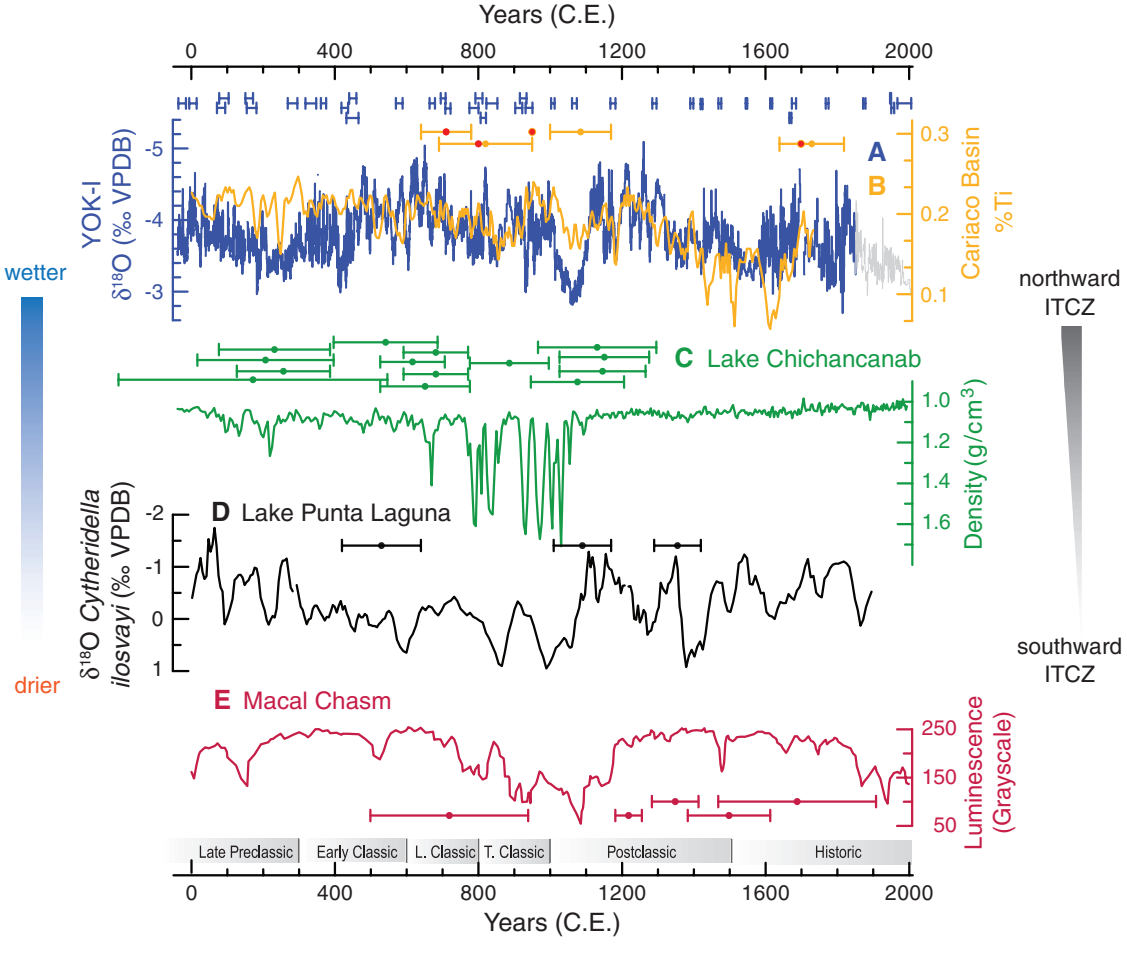

Fig. 1. Comparison of (**A**) stalagmite YOK-I $\delta^{18}O$ with (**B**) Tuned (red dots) (*10*) bulk sediment titanium record from the Cariaco Basin, Venezuela (*11*). (**C**) Lake Chichancanab sediment density record (*12*). (**D**) Lake Punta Laguna ostracod (*Cytheridella ilosvayi*) $\delta^{18}O$ record (*13*). (**E**) Macal Chasm speleothem luminescence record (*8*). Similarities in the YOK-I and Cariaco records suggest that rainfall variability was strongly modulated by ITCZ migration. Age models for each record are based on calibrated ^{14}C or U-Th, with error bars showing the relative chronological precision of each record. Smoothed records that emphasize multidecadal trends are shown in fig. S17. The light gray line denotes uncertainties in the 20th- century $\delta^{18}O$ record (details and climate archive locations are available in the supplementary materials).

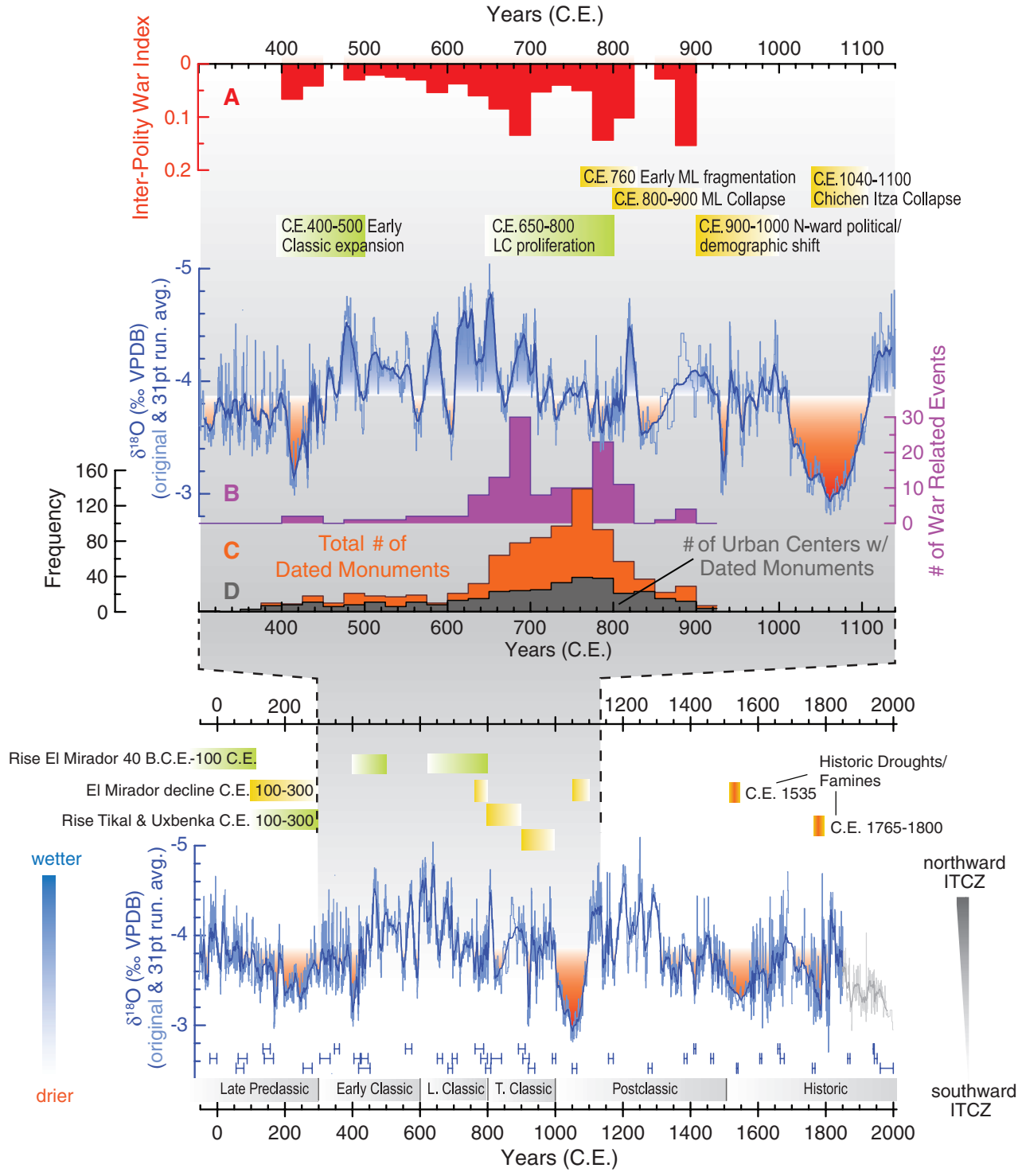

Fig. 2. (Bottom) YOK-I $\delta^{18}O$ climate record spanning the past 2000 years (40 B.C.E. to 2006 C.E.) shown relative to Maya chronology and major historical events. Blue bars just below the $\delta^{18}O$ curve indicate the small error for each of the 40 U-Th dates used to constrain the chronology of the $\delta^{18}O$ climate record (*10*). Drier-than-average conditions during this interval are shown in orange. Two historically recorded droughts in the 16th- and 18th-century C.E. accord well with the YOK-I record, and the earliest multidecadal drought in the record (200 to 300 C.E.) corresponds with decline of the large center of El Mirador and a major sociopolitical reorganization in the ML. (Top) The YOK-I $\delta^{18}O$ climate record between 300 and 1140 C.E. shown relative to major historic events along with (**A**) An interpolity warfare index based on the number of war-related events between Maya sites or rulers relative to the total number of events recorded during each interval. (**B**) Raw number of war-related events. (**C**) Frequency distribution of long-count dated monuments in the ML. (**D**) Total number of urban centers with dated monuments through time as a proxy for the development and disintegration of complex polities in the ML. All hieroglyphic data are from the Maya Hieroglyphic database (raw data is available in the supplementary materials) (*28*) and are binned in 25-year intervals. The light gray line denotes uncertainties in the 20th-century $\delta^{18}O$ record (*10*).

at the end of the Preclassic Period (200 to 300 C.E.). Maya populations had expanded across the ML during the Middle and Late Preclassic Periods (1000 B.C.E. to 100 C.E.), exploiting productive agricultural soils and seasonal wetlands (*16, 17*). Multiple fully developed polities emerged in the ML (*18*), including the large center of El Mirador in northern Guatemala (*19*). The drying trend evident in the YOK-I record starting at 100 C.E. culminated in a century-long dry interval (200 to 300 C.E.) that corresponds to the demise of El Mirador, which is consistent with the hypothesis that drought played a role in the political realignment and reorganization of ML population centers between 150 to 300 C.E. (*12*). Several ML polities persisted, however, and became more integrated and grew in size, including Uxbenká (*20*).

Tikal, already established in the central Peten (Guatemala) as an important regional center during the Middle and Late Preclassic (1000 B.C.E. to 300 C.E.), emerged as a dominant sociopolitical force in the wake of the climatic and social instability of the 3rd and 4th centuries C.E. (*21*). Tikal, Calakmul, and other important sites in the central Peten were positioned near seasonal wetlands under intensive use (*22*). High rainfall during the Early Classic evident in the YOK-I record (Fig. 2) maintained these wetlands and seasonally recharged constructed water storage systems (reservoirs and tanks) (*23*). This helps to explain the growing geopolitical influence of polities like Tikal, Calakmul, Caracol, and Naranjo. Many of the best-recorded ruling Maya lineages were founded around 440 to 500 C.E. (*24*) during this interval of anomalously high rainfall. The overall number of monument-bearing political centers and indications of war among them also increased throughout the Early Classic (300 to 650 C.E.) (Fig. 2).

Terminal Classic Period droughts have been cited as causes of societal collapse in the Maya lowlands (*1*). The YOK-I record is consistent with this hypothesis, showing a multidecadal drought at this time (820 to 870 C.E.). This finding is consistent with arguments for a ~40% reduction in summer rainfall during the Terminal Classic Period (*9*). Multidecadal drought between 820 and 870 C.E. was part of a broader regional drying trend starting 640 C.E., culminating at 1020 C.E. in a century-long dry period that is the most pronounced in our record. The early stages of this drying trend correspond with an increase in interpolity warfare (Fig. 2, A and B) and expansion in the number of competing political centers, enumerated here from long count-dated historical texts (Fig. 2, C and D, and tables S7 and S8). War-related events increased during a dry interval between 640 and 660 C.E., but then peaked after a lag during a wetter interval between 660 and 700 C.E. Climate drying after 640 C.E. may have exacerbated environmental degradation that occurred with 5th- and 6th-century C.E. population expansion under a wetter climatic regime. Drying constrained agricultural productivity, stimulated inter-polity warfare (*25*), and promoted political competition and fissioning that was ultimately unsustainable.

The first evidence for political fragmentation occurred in the Petexbatun region between 760 and 800 C.E. (*26*), corresponding with a dry interval in the YOK-I record, peak population densities throughout the region (145 people per km^2) (*27*), and the maximum spatial extent of monument-bearing urban centers (Fig. 2, C and D). Historical texts on stone monuments were dedicated in at least 39 centers from 750 to 775 C.E., with rulers commissioning monuments at several large centers at unprecedented rates. These texts point to a dynamic and unstable geopolitical landscape centered on status rivalry, war, and strategic alliances (*28*). A precipitous drop in the number of texts at key centers (such as Tikal) between 775 and 800 C.E. was the precursor to a 50% drop in the number of centers with text-dated monuments between 800 and 825 C.E., which is evidence for widespread failure of these political systems. Increasing interpolity warfare (Fig. 2A) is most evident in the historical record between 780 and 800 C.E. Political power became decentralized as the institution of divine kingship collapsed between 780 and 900 C.E. Less is known about the fate of the people integrated into these polities, but depopulation took centuries and entailed migration, reorganization (*29*, *30*), and persistence in the environs surrounding abandoned cities (such as Mopan Valley, Guatemala) (*21*). Centers of political importance shifted to the northern parts of the Yucatan Peninsula as carved stone monuments were commissioned less frequently in the central Peten; the tradition ended at Chichen Itza sometime between 1000 and 1100 C.E. during the longest and driest interval of the past 2000 years.

ITCZ migration–influenced climate variability in the ML as recorded in YOK-I aids in understanding the complex socio-natural processes associated with Maya political dynamics during the past 2000 years. Population increases and the expansion of Classic Maya polities were favored by anomalously high rainfall and increased agricultural productivity between 440 and 660 C.E. High-density Maya populations were increasingly susceptible to the agricultural consequences of climate drying. We propose that a two-stage collapse commenced with the 660 C.E. drying trend. It triggered the balkanization of polities, increased warfare, and abetted overall sociopolitical destabilization. Political disintegration in the Petexbatun region foreshadows two multidecadal dry intervals that further reduced agricultural yields and caused more widespread political disintegration between 800 and 900 C.E. This was followed by a second stage of more gradual population decline and then punctuated population reductions during the most extreme dry interval in the YOK-I record between 1020 and 1100 C.E. The linkage between extended 16th-century drought, crop failures, death, famine, and migration in Mexico provides a historic analog evident in the YOK-I record for the sociopolitical tragedy and human suffering experienced by the 11th-century Maya. It also helps explain why the cultural elaboration evident during the Classic Period never fully redeveloped.

References and Notes

1. D. A. Hodell, J. H. Curtis, M. Brenner, *Nature* **375**, 391 (1995).
2. G. H. Haug *et al.*, *Science* **299**, 1731 (2003).
3. S. E. Metcalfe, M. D. Jones, S. J. Davies, A. Noren, A. MacKenzie, *Holocene* **20**, 1195 (2010).
4. D. W. Stahle *et al.*, *Geophys. Res. Lett.* **38**, L05703 (2011).
5. M. S. Lachniet, J. P. Bernal, Y. Asmerom, V. Polyak, D. Piperno, *Geology* **40**, 259 (2012).
6. J. Aimers, D. Hodell, *Nature* **479**, 44 (2011).
7. A. B. Frappier, D. Sahagian, S. J. Carpenter, L. A. González, B. R. Frappier, *Geology* **35**, 111 (2007).
8. J. W. Webster *et al.*, *Palaeogeogr. Palaeoclimatol. Palaeoecol.* **250**, 1 (2007).
9. M. Medina-Elizalde, E. J. Rohling, *Science* **335**, 956 (2012).
10. Materials and methods are available as supplementary material on *Science* Online.
11. G. H. Haug, K. A. Hughen, D. M. Sigman, L. C. Peterson, U. Röhl, *Science* **293**, 1304 (2001).
12. D. A. Hodell, M. Brenner, J. H. Curtis, *Quat. Sci. Rev.* **24**, 1413 (2005).
13. J. H. Curtis, D. A. Hodell, M. Brenner, *Quat. Res.* **46**, 37 (1996).
14. B. Mendoza, V. García-Acosta, V. Velasco, E. Jáuregui, R. Díaz-Sandoval, *Clim. Change* **83**, 151 (2007).
15. V. García-Acosta, J. M. Pérez-Zevallos, A. Molina del Villar, *Desastres Agrícolas en México. Catálogo Histórico. Tomo I: Épocas Prehispánica y Colonial* (Fondo de Cultura Económica and CIESAS, México, 2003), pp. 958–1822.
16. N. P. Dunning *et al.*, *Ann. Assoc. Am. Geogr.* **92**, 267 (2002).
17. S. Luzzadder-Beach, T. P. Beach, N. P. Dunning, *Proc. Natl. Acad. Sci. U.S.A.* **109**, 3646 (2012).
18. F. Estrada-Belli, *The First Maya Civilization: Ritual and Power Before the Classic Period* (Routledge, London, 2011).
19. R. D. Hansen, S. Bozarth, J. Jacob, D. Wahl, T. Schreiner, *Ancient Mesoamerica* **13**, 273 (2002).
20. B. J. Culleton, K. M. Prufer, D. J. Kennett, *J. Archeologic. Sci.* **39**, 1572 (2012).
21. J. P. Laporte, V. Fialko, *Ancient Mesoamerica* **6**, 41 (1995).
22. T. Beach *et al.*, *Quat. Sci. Rev.* **28**, 1710 (2009).
23. V. L. Scarborough *et al.*, *Proc. Natl. Acad. Sci. U.S.A.* **109**, 12408 (2012).
24. S. Martin, N. Grube, *Chronicle of the Maya Kings and Queens* (Thames & Hudson, London, 2008).
25. D. Webster, *The Fall of the Ancient Maya: Solving the Mystery of the Maya Collapse* (Thames and Hudson, London, 2002).
26. A. Demarest, *Ancient Maya: The Rise and Fall of a Rainforest Civilization* (Cambridge Univ. Press, Cambridge, 2004).
27. T. P. Culbert, D. S. Rice, Eds., *Precolumbian Population History in the Maya Lowlands* (Univ. of New Mexico Press, Albuquerque, 1990).
28. J. L. Munson, M. J. Macri, *J. Anthropol. Archaeol.* **28**, 424 (2009).
29. J. A. Sabloff, *Proc. Am. Philos. Soc.* **151**, 11 (2007).
30. P. M. Rice, D. S. Rice, in *The Terminal Classic in the Maya Lowlands: Collapse, Transition, and Transformation*, A. A. Demarest, P. M. Rice, D. S. Rice, Eds. (Univ. Press of Colorado, Boulder, CO, 2004), pp. 125–139.

Acknowledgments: We thank D. Hodell, M. Brenner, J. Yaeger, J. Lohse, J. Kennett, D. Webster, and three anonymous reviewers for their useful comments. Thanks to H. Meyer (AWI Potsdam for isotope analysis of rain and drip water. This research was supported by NSF (HSD-0827305, BCS-0940744, and EAR-0326902), European Research Council (240167), Swiss National Foundation (CRSI22-132646/1), the German Science Foundation (DFG FOR1380 "HIMPAC"), and the Alphawood Foundation.

Supplementary Materials

www.sciencemag.org/cgi/content/full/338/6108/788/DC1
Materials and Methods
Figs. S1 to S17
Tables S1 to S8
References (*31–211*)

19 June 2012; accepted 26 September 2012
10.1126/science.1226299